RESEARCH

Effect of moisture content on the rockburst intensity of sandstones

Jianchao Wang · Wei Wang · Guoqing Chen · Yanke Wang

Abstract Rockburst is a common geological hazard in deep underground engineering, and it often occurs in strata consisting of brittle rocks. In this study, the moisture content effect on the rockburst intensity of sandstones is systematically studied. A series of triaxial unloading compression tests along with the acoustic emission monitoring are performed for sandstone specimens with different moisture content levels. The mechanical properties, failure characteristics, and dilatancy behaviors of sandstone specimens are then properly compared. Comparative results reveal that the triaxial compressive strength and total strain energy of the saturated specimen decrease by about 30% and 35%, respectively, as compared to those of the dry specimen. Moreover, the magnitude of elastic strain energy tends to decrease with the increasing water content. The effect of moisture content on the rockburst intensity of sandstones is, therefore, significant. Besides, it is also found that the onset of dilatancy is generally unaffected by the water content, whereas the extent of dilatancy significantly decreases with the increasing water content. Numerical simulations for a tunnel excavation model confirm that injecting water into the surrounding rock is an effective way of reducing the rockburst intensity during tunnel excavations. These results have a guiding significance for the prevention and control of rockbursts in underground engineering.

Article Highlights

(1) Triaxial unloading compression tests are conducted on sandstone specimens with various confining pressure and moisture content levels.
(2) The moisture content effect on the mechanical properties, failure characteristics, and dilatancy behaviors of sandstones are studied.
(3) A numerical tunnel excavation case confirms that injecting water into the surrounding rock composed of sandstones can reduce the rockburst intensity.

J. Wang · G. Chen · Y. Wang
State Key Laboratory of Geohazard Prevention and Geoenvironment Protection, Chengdu University of Technology, 1, Dongsanlu, Erxianqiao, Chengdu 610059, Sichuan, People's Republic of China

W. Wang (✉)
State Key Laboratory of Simulation and Regulation of Water Cycle in River Basin, China Institute of Water Resources and Hydropower Research, A1 Fuxing Road, Haidian 100038, Beijing, People's Republic of China
e-mail: wangw_cdut@126.com

1 Introduction

Rockburst is a common geological hazard during the excavation process of underground engineering under high geo-stress conditions (Zhang et al. 2012; Zhou et al. 2015; Guo et al. 2017). Excavations might lead to the stress release of brittle surrounding rocks, which in turn yields the energy release of rocks, thus resulting in a rockburst hazard in terms of the loosening, spalling, and ejection of rock fragments (Li et al. 2012a, b; Xiao et al. 2016; Gu et al. 2023). Because of their sudden and highly destructive characteristics, rockburst hazards seriously threaten the safety of constructors and equipments (Feng et al. 2015; Liang et al. 2019) as well as the stability of supporting structures (Feng et al. 2016; Wang et al. 2019). Considering the increasing number of tunnels constructed under high geo-stress conditions in the recent decade, it is of high significance to investigate the mechanism of rockbursts, in order to minimize the losses caused by the rockburst hazards.

Sandstone is a medium-grained clastic sedimentary rock, which is often encountered during tunnel excavations. On one hand, to the authors's knowledge, the mechanical properties of sandstones are strongly affected by moisture (Hawkins and McConnell 1992; Baud et al. 2000; Vásárhelyi and Ván, 2006; Kim and Changani 2016; Wong et al. 2016; Tang 2018). Baud et al. (2000) found that the reductions of brittle strength of wet sandstones range from 5 to 17%. Based on the data collected from uniaxial compressive loading experiments of sandstones, Tang (2018) proposed exponential equations to describe the relationships of strength, Poisson's ratio, and elastic modulus versus soaking duration, respectively. On the other hand, due to the relatively high brittleness of sandstones (Chen et al. 2017a, b), rockbursts would possibly occur when an excavation chamber passes through a sandstone stratum. Yet, only a few studies (Liu et al. 2018) exist investigating the influence of moisture content on the rockburst characteristics of sandstones. Liu et al. (2018) tracked the rockburst process via acoustic emission (AE) and infrared thermal imager monitoring systems, and they reported that dry and saturated conditions is likely to yield spalling and V-shape fracture zones, respectively.

The influence of moisture on mechanical properties and fracture behaviors of sandstones have been widely studied by means of various laboratory experiments, including uniaxial compression test (Shen et al. 2020; Luo 2020), triaxial compression test (Li et al. 2012a, b; Chen et al. 2017b; Feng et al. 2020), Brazilian splitting test (Huang et al. 2020), and notched semi-circular bending test (Zhou et al. 2018). For instance, Huang et al.(2020) found that the uniaxial compression and triaxial compression strengths of a clay-bearing red sandstone decrease by about 53% and 29%, respectively, when the water saturation changes from 0 to 1. However, triaxial unloading compression tests tend to be more consistent with the actual stress path of the surrounding rock (Huang et al. 2001; Huang and Li 2014; Li et al. 2017). Therefore, more research efforts should be made on the basis of the triaxial unloading compression test. In addition, the advanced numerical simulation has been increasingly utilized in underground engineerings over the past decade (Song et al. 2014; Tang et al. 2018; Tian et al. 2021), which provides an effective way of reproducing the brittleness and rockburst characteristics of sandstones.

The aim of this study is to investigate the effect of water content on the rockburst intensity of sandstones. A series of triaxial unloading compression tests are performed for sandstones with varying water content levels. Based on the experimental results, the mechanical properties, failure characteristics, and dilatancy behaviors of sandstone specimens are subsequently compared, in order to scrutinize the water content effect on the rockburst intensity. Such effect is further verified by conducting numerical analysis of a tunnel excavation model implemented in $RFPA^{2D}$ (Tian et al. 2021). This research provides valuable insights into the mechanism of moisture content effect on the rockburst intensity of sandstones.

2 Specimen preparations and test methods

2.1 Specimen preparations

The rock samples used are collected from the sandstone stratum of Bamiao tunnel in Bazhong, Sichuan Province, China. Figure 1 shows the location and excavation situations of this tunnel. Several times of rockburst hazards have occurred in this tunnel, causing severe damages to the initial support (see Fig. 1b). To reduce the losses caused by rockburs, many effective measures have been taken, such as injecting water

Fig. 1 **a** Location of Bamiao tunnel; **b** damage of the initial support caused by rockburst hazards; and **c** spraying water onto the surface of surrounding rocks
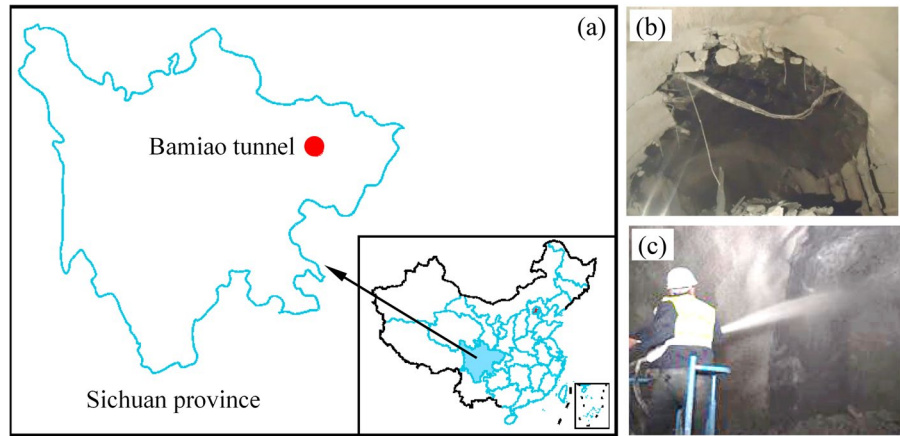
into the surrounding rocks before tunnel excavations (see Fig. 1c).

The mineral compositions of the sandstone samples are mainly quartz and illite, with a small amount of silicate and clay. The average density and porosity of these samples are 2.6 g/cm^3 and 0.09, respectively. According to the methods suggested by International Society for Rock Mechanics (ISRM 2015), all samples are processed into cylinders with a diameter of 50 mm and a length of 100 mm. To investigate the effect of water content on the mechanical properties and failure characteristics of the sandstone, these samples are devided into 5 groups with the water saturation coefficient (K_s) being 0.0, 0.25, 0.50, 0.75, and 1.0, respectively. K_s is expressed as:

$$K_s = w_a/w_{sa} \tag{1}$$

in which w_a and w_{sa} are the actual moisture content and saturated moisture content of rock samples, respectively. One can refer to Chen et al. (2017a) for the detailed method of controlling the K_s value of a sandstone specimen.

2.2 Test methods

To obtain stress–strain curves of sandstones, a series of triaxial unloading compression tests are performed. For comparison, triaxial compression tests are also conducted. Both types of tests are performed in MTS815. MTS815 is an experimental equipment for rock materials, capable of precisely tracking the load, pressure, and deformation of specimens. Three levels of confining stresses, namely 20, 30, and 40 MPa, are considered, and three times of compression tests are repeated for each confining stress level. Therefore, the total number of tests is 90 (2 test methods $\times$ 5 water

Fig. 2 Schematic diagrams of the loading paths for **a** the triaxial compression test, and **b** the triaxial unloading compression test. Note that σ_1 and σ_3 denote the axial and confining pressures, respectively
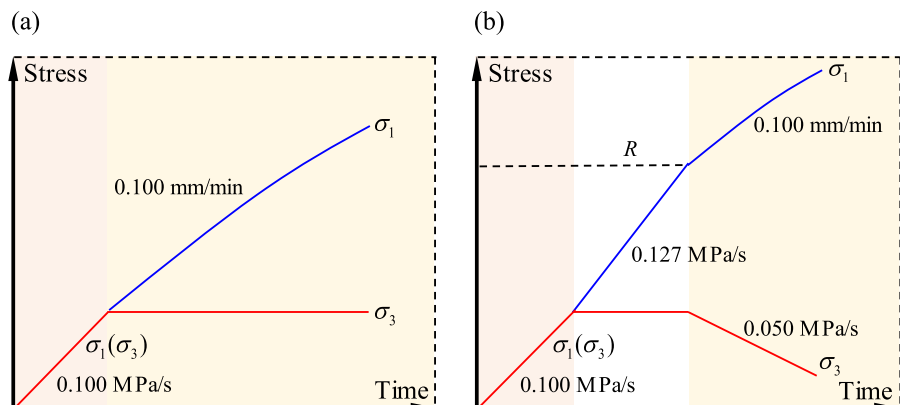
saturation coefficient values×3 confining stress levels×3 repeated times).

Figure 2 schematically illustrates the loading paths of both test methods. The steps of performing the triaxial compression test are summarized as follows:

(1) Apply axial and confining pressures simultaneously at a loading rate of 0.100 MPa/s.
(2) When both pressures reach a designed confining stress level, fix the confining pressure, and continually apply the axial pressure with a rate of 0.100 mm/min until the rock specimen is completely damaged.

On the other hand, the steps of performing the triaxial unloading compression test are described as follows:

(1) Apply axial and confining pressures simultaneously at a loading rate of 0.100 MPa/s.
(2) When both pressures reach a designed confining stress level, keep the confining pressure, and continually apply the axial pressure with a rate of 0.127 MPa/s (i.e., 1.0 kN/s).
(3) When the axial pressure reaches a target value R, relieve the confining pressure at an unloading rate of 0.050 MPa/s, and continually apply the axial pressure with a rate of 0.100 mm/min until the rock sample is completely damaged. Note that R denotes 0.8 times of the compressive strength of rock samples in the triaxial compression test; the R values for different combinations of confining stress and moisture content levels are tabulated in Table 1.

Table 1 Target axial pressures for the rock specimens with different confining stress and water saturation coefficient levels. (unit: MPa)

Confining stresss (MPa)	Water saturation coefficient				
	0.00	0.25	0.50	0.75	1.00
20	233.60	213.60	199.20	189.60	175.20
30	279.20	244.00	236.80	224.00	200.00
40	320.00	292.80	269.60	253.60	232.80

3 Experimental results

3.1 Rockburst mechanism based on the conversion of strain energy

During laboratory tests, the work done by experimental equipments is converted to the strain energy (U) of specimens through specimen deformations. U can be divied into two parts (Chen et al. 2019; Zhang et al. 2019a):

$$U = U_d + U_e \tag{2}$$

where U_d denotes the dissipation energy, which describes the energy dissipated in the process of plastic deformations and crack growths; and U_e represents the elastic strain energy, which characterizes the energy stored during the process of elastic deformations. For the laboratory tests conducted herein, U and U_e can be estimated through the following equations, respectively (Chen et al. 2017a):

$$U = \int \sigma_1 d\varepsilon_1 + 2 \int \sigma_3 d\varepsilon_3 \tag{3}$$

$$U_e = \frac{1}{2E} \left[\sigma_1^2 + 2\sigma_3^2 - 2\mu(\sigma_3^2 + 2\sigma_1\sigma_3) \right] \tag{4}$$

in which σ_1 and σ_3 stand for the maximum principal stress (i.e., axial stress) and the minimum principal stress (i.e., confining stress), respectively; ε_1 and ε_3 represent the maximum principal strain (i.e., axial strain) and the minimum principal strain (i.e., lateral strain), respectively; and E and μ denote the Young's modulus and Poisson's ratio, respectively.

When a brittle rock failure occurs, U_e is partly converted to the kinetic energy of rock fragments, thus resulting in a rockburst. Such kinetic energy is generally referred to as energy difference (ΔU) in existing studies (Zhu et al. 2007; Chen et al. 2009; Xue et al. 2021), and can be computed by the following equation:

$$\Delta U = U_e - U_c \tag{5}$$

where U_c is the limit storage energy, which specifies the minimum U_e needed for the occurrence of rockbursts. For a specified rock type, U_c remains constant given different stress paths, and can be calculated as follows:

$$U_c = \frac{\sigma_c^2}{2E} \qquad (6)$$

in which σ_c denotes the uniaxial compressive strength. Therefore, a rockburst occur only when $U_e > U_c$, and the rockburst intensity is proportional to the magnitude of U_e (or ΔU).

3.2 Effect of moisture content on mechanical properties

Figure 3 compares the deviatoric stress–strian curves obtained from the triaxial compression and triaxial unloading compression tests under the confining stress of 30 MPa and the saturation coefficients of 0.0, 0.5, and 1.0. According to the existing studies (Martin and Chandler 1994; Alkan et al. 2007; Peng et al. 2019), prior to the peak stress, a stress-strian curve can be divided into four main stages, as schematically illustrated in the right-side plot. Two observations can be made. First, as expected, the peak deviatoric stresses of the triaxial unloading compression test are notably smaller than those of the triaxial compression test. Second, the peak deviatoric stress decreases noticeably with the increasing water saturation coefficient, indicating a weakening effect of water on the compressive strength of specimens.

For demonstration purpose, Fig. 4 displays the deviatoric stress-strian curves produced by the triaxial unloading compression tests. Figure 5 compares the dependences of the peak deviatoric stress on the water saturation coefficient under different confining stress levels. It clearly shows that the peak deviatoric stress is inversely proportional to the water saturation coefficient. Taking the confining stress of 30 MPa for example, the peak stress of the saturated specimen is reduced by about 30%, as compared to that of the completely dry specimen. To the authors's knowledge, there are three main reasons for such strength loss (i.e., decrease of the peak deviatoric stress). First, the component of clay minerals in the sandstone samples exhibits a strain-softening behavior, which is highly sensitive to the moisture content (Hawkins and McConnell 1992). Second, the tensile force of water reduces the cohesion between different grains, thus promoting the propagation of micro-cracks (Lu et al. 2019; Liu et al. 2023). Third, the water wedge effect caused by pore water pressure also promotes the propagation of micro-cracks (Zhou et al. 2018). Therefore, as shown in Figs. 3, 4, and 5, it is evident that a higher moisture content is likely to yield a smaller compressive strength of sandstones.

The effect of the moisture content on the Poisson's ratio of rock specimens is also investigated. Poisson's ratio reflects the elastic deformation characteristics of
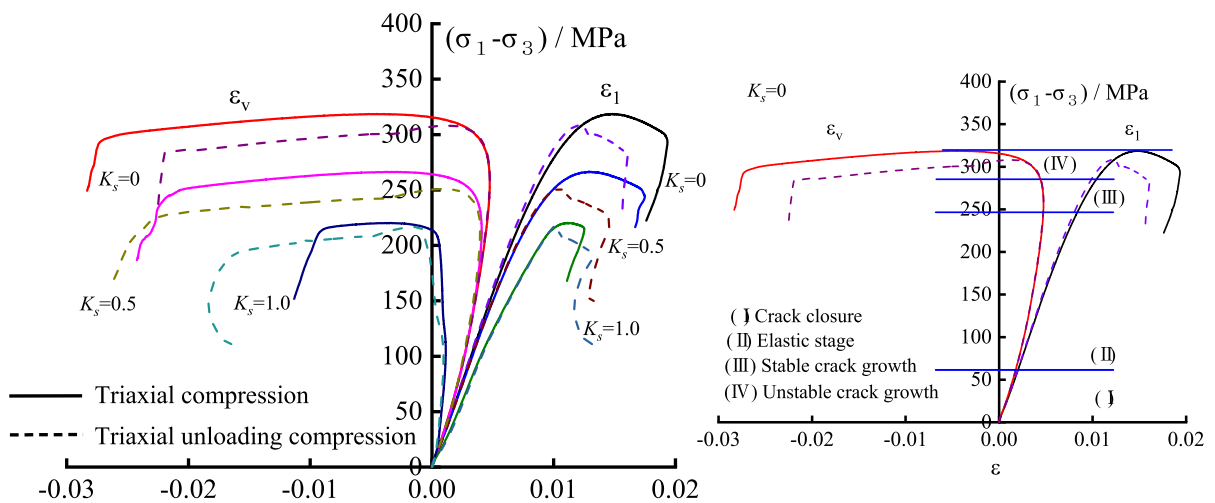

Fig. 3 Comparison of the deviatoric stress–strain curves obtained from the triaxial compression and triaxial unloading compression tests given the confining stress being 30 MPa and the water saturation coefficient being 0.0, 0.5, and 1.0. Note that ε_1 and ε_v represent the axial and volumetric strains, respectively; and the right-side schematic plot is provided to demonstrate four main stages of deviatoric stress-strian curves
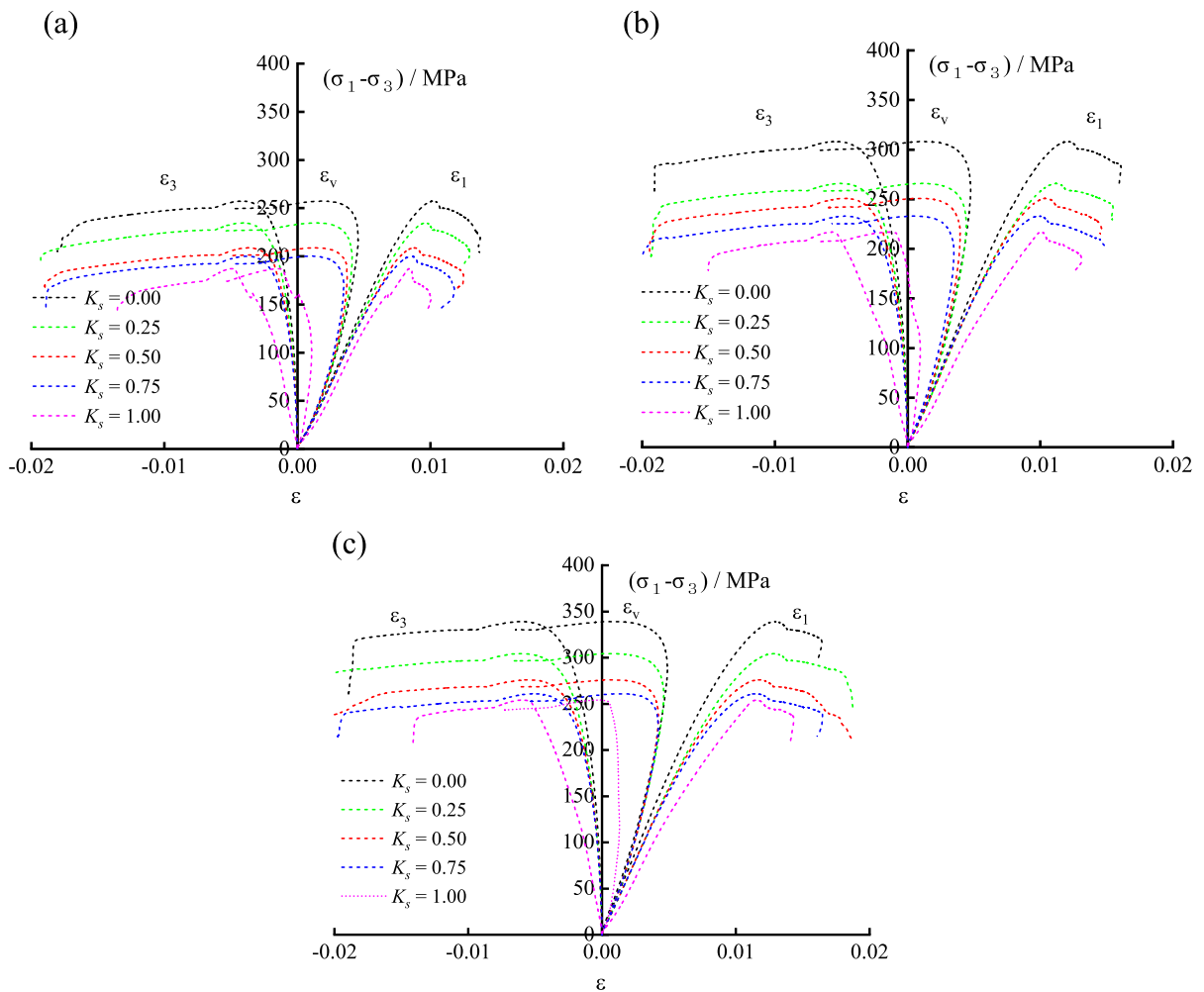
(a)

(b)

(c)

Fig. 4 Deviatoric stress–strain curves obtained from the triaxial unloading compression test with the confining pressure being **a** 20 MPa, **b** 30 MPa, and **c** 40 MPa, respectively. Note that ε_1, ε_3, and ε_v represent the axial, lateral, and volumetric strains, respectively

materials, and it is determined herein by the ratio of the lateral strain increment to the axial strain increment in the elastic stage. Figure 6 illustrates the dependences of Poisson's ratio on the water saturation coefficient under different test conditions. It is seen that Poisson's ratio tends to increase with the increasing saturation coefficient. Moreover, Poisson's ratios of the specimens with $K_s = 1.0$ are dramatically larger, as compared with those of the specimens with remaining K_s values. Considering the Poisson's ratios of air and water are 0.0 and 0.5, respectively, and the air in rock voids is gradually replaced by water (with increasing K_s), it is not surprising to see the increasing trend of Poisson's ratio of rock specimens. When

$K_s = 1.0$, the rock voids are completely filled with water, and thus the lateral deformation of specimens can not be offset by the rock voids, which subsequently yields a dramatically larger Poisson's ratio of rock specimens. Therefore, a higher moisture content tends to cause a larger Poisson's ratio of sandstones, especially when $K_s = 1.0$.

As can be seen in Eqs. (3 and 4), both the peak axial stress and Poisson's ratio play roles in energy evolutions. Thus, the effect of the moisture content on the energy-related parameters is further examined. Figure 7a and b illustrates the elastic strain energy and the dissipation energy, respectively, as a function of the water saturation coefficient under
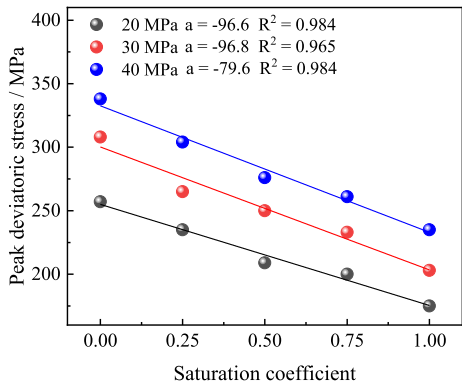
Fig. 5 Dependences of the peak deviatoric stress on the saturation coefficient given various confining stresses. Note that *a* and R^2 represent the slope and the coefficient of determination of the fitted lines, respectively
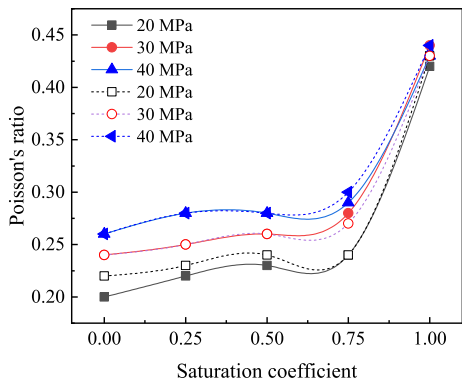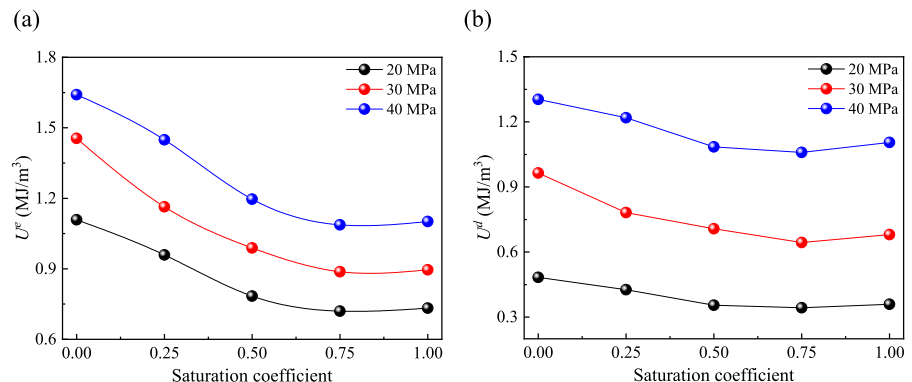

Fig. 6 Dependences of Poisson's ratio on the saturation coefficient under different test methods and confining stresses. Note that the dashed and solid lines denote the triaxial compression and triaxial unloading compression tests, respectively

various confining stresses. Figure 8 shows their proportions relative to the total strain energy (i.e., normalized values) accordingly. Note that both plots are on the basis of the triaxial unloading compression test. Several observations can be drawn. First, as the saturation coefficient increases, the elastic strain energy decreases for a given confining stress, indicating that increasing the water content significantly decreases the storage capacity of the elastic strain energy. Second, although the dissipation energy tends to decrease with the increasing saturation coefficient, the normalized dissipation energy generally increases with the increasing saturation coefficient. This is not unexpected, since the total energy decreases with the increasing saturation coefficient. Taking the confining stress of 30 MPa as an example, the magnitude of total strain energy decreases by about 35% as K_s changes from 0.0 to 1.0. Thus, as the water content increases, more input work is converted to the energy used for the initiation and extension of micro-cracks. Third, the confining stress exhibits a significantly larger amplification effect on dissipation energy, as compared with the elastic strain energy. These observations imply that both effects of the moisture content and confining stress on the energy evolution of sandstones are significant.

3.3 Effect of moisture content on failure characteristics

There are two types of fracture surfaces in a completely failure rock specimen, namely the tension fracture surface and the shear fracture surface. In general, the tension fracture surface is nearly vertical

Fig. 7 Comparisons of **a** the elastic strain energy and **b** the dissipation energy under different confining stresses against the saturation coefficient

Fig. 8 Comparisons of **a** normalized elastic strain energy and **b** normalized dissipation energy versus the water saturation coefficient given different confining stresses
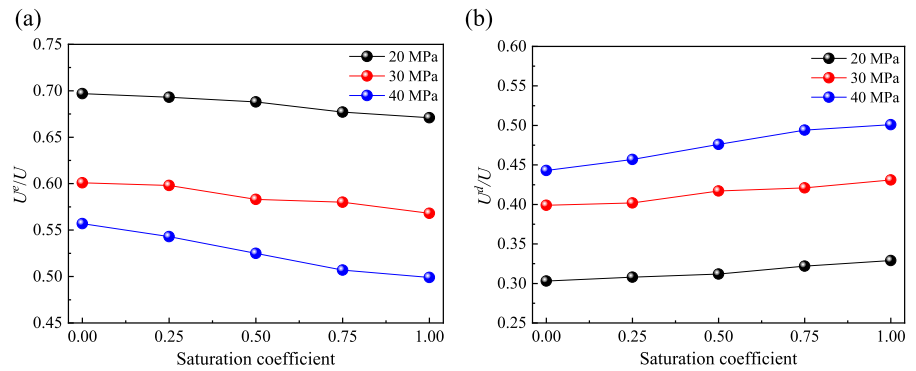
in angle with few powder particles on the surface, whereas the shear fracture surface is approximately 45° in angle with quite a number of powder particles on the surface. Moreover, as the brittleness of rock specimens increases (i.e., larger elastic strain energy and smaller dissipation energy), more tension fracture surfaces tend to be formed (Zhang et al. 2019b). Figure 9 compares the fracture surfaces of sandstone specimens from the triaxial unloading compression test. As shown in this plot, both types of fracture surfaces exist when $K_s = 0.0$ and 0.25, but only shear fracture surface is formed when $K_s = 0.5$, 0.75, and 1.0. Considering the correlation between the brittleness of rock specimens and the number of tension fracture surfaces, it is clear that increasing the water content significantly weakens the brittleness of sandstone specimens (i.e., smaller elastic strain energy and larger dissipation energy).

The AE count rate can reflect the activity level of micro-cracks in a rock specimen, thus reflecting the evolution process of rock failure. The dominant frequency and amplitude of AE signals reflect the size of micro cracks in a rock specimen. Figure 10 compares the AE count rate and deviatoric stress against the elapsed time for the sandstone specimens with an identical confining stress yet different water saturation coefficients. It is seen that the AE signals for the specimen with $K_s = 0.0$ are broadly in a concave shape. As for the specimens with $K_s = 0.5$ and 1.0, the distribution of AE signals tends to be more uniform. Besides, as the water saturation coefficient increases, the density and intensity of the AE count rate during the period of rock failure (i.e., the elapsed time being about 3500–4500 s) become smaller, indicating that the released energy in the period of rock failure decreases with the increasing water content. Figure 11
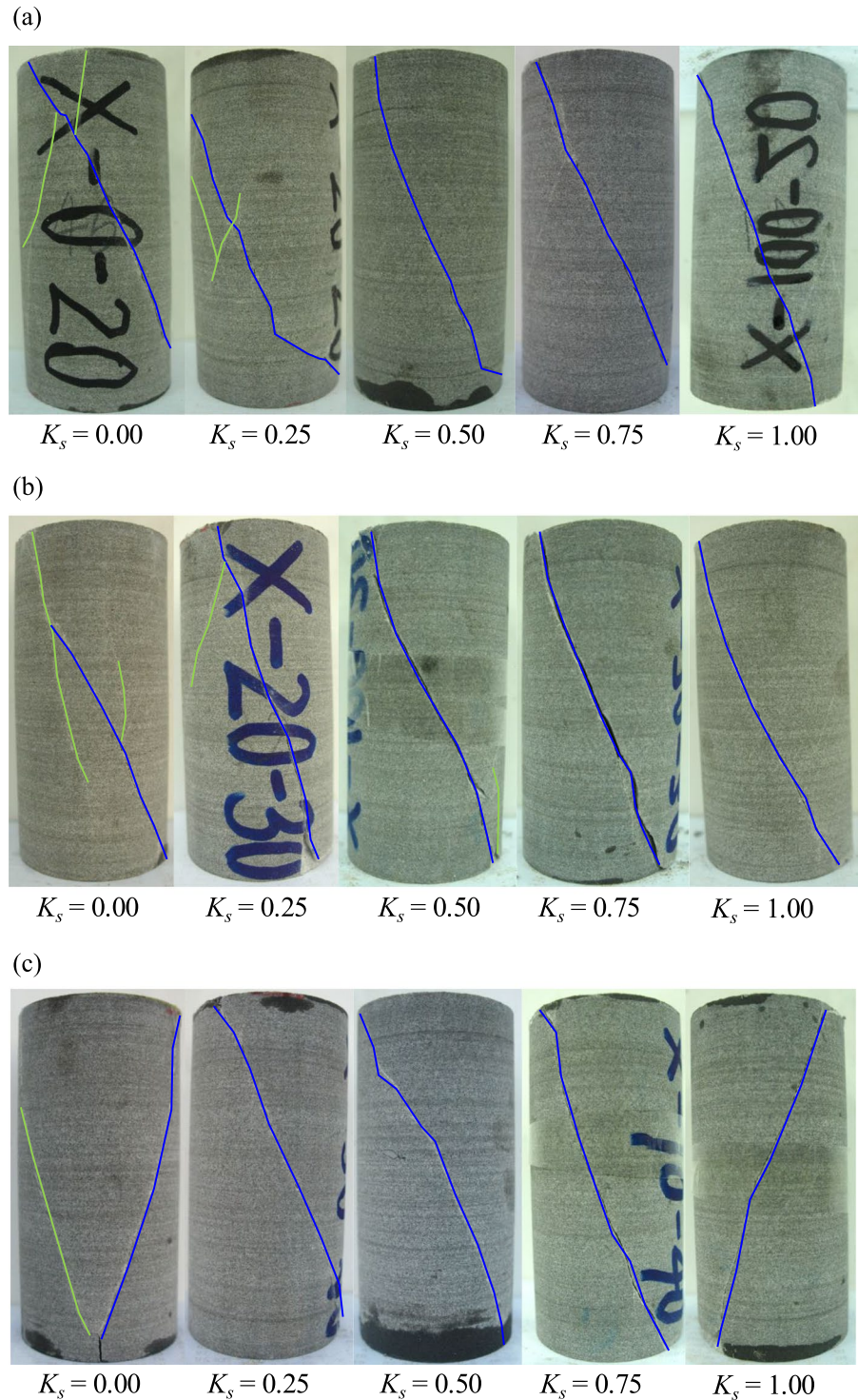
illustrates the distributions of dominant frequency and amplitude of AE signals against the elapsed time. As shown in this plot, during the period of rock failure, the occurence of AE signals with high dominant frequencies (> 200 Hz) and high amplitudes tends to decrease with increasing water saturation coefficients, indicating that smaller micro-cracks would possibly be formed given a higher water content of sandstone specimens. Therefore, as shown in Figs. 9, 10 and 11, it is clear that a higher moisture content is likely to cause a lower brittleness of sandstones.

3.4 Effect of moisture content on dilatancy behaviors

An increase in volume during the process of rock deformations is called dilatancy. The onset of dilatancy marks the beginning of stage IV (see Fig. 3), in which irreversible cracks continuously expand and the dissipation energy significantly increases (Yang et al. 2017; Zhang et al. 2019b). The stress level corresponding to the onset of dilatancy is referred to as crack-damage stress (σ_{cd}), and can be identified from non-linearity in either the deviatoric stress against volumetric strain curve or the volumetric strain versus axial strain curve as recorded during experiments (Yuan and Harrison 2004).

Figure 12 compares the deviatoric stress as functions of the axial and volumetric strains, respectively, from the triaxial unloading compression test. It is seen that both crack-damage stress and peak stress decrease with the increasing water saturation coefficient. Moreover, the ratios of the crack-damage stress to the peak stress are 0.86, 0.85, 0.84, 0.83, and 0.44 for $K_s = 0.0$, 0.25, 0.5, 0.75, and 1.0, respectively. These ratios are comparable except 0.44, indicating that

Fig. 9 Comparisons of the failure modes of sandstone specimens with different moisture contents under the confining pressures of **a** 20 MPa, **b** 30 MPa, and **c** 40 MPa, respectively. Note that the green and blue lines denote the tension and shear fractures, respectively
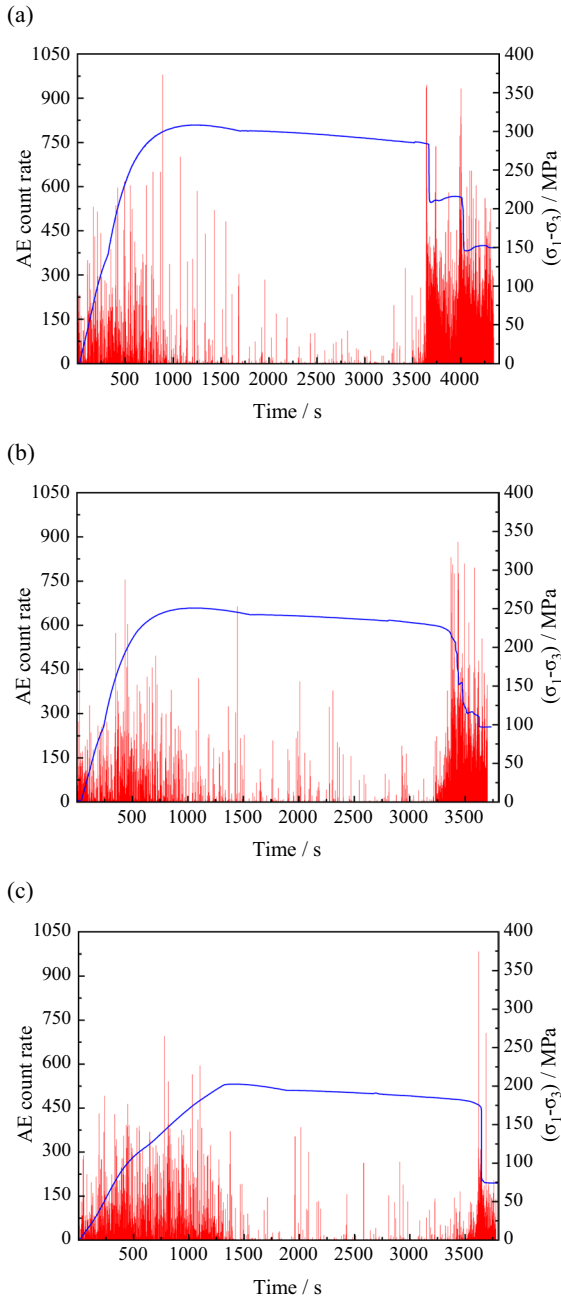

(a)

$K_s = 0.00$ $K_s = 0.25$ $K_s = 0.50$ $K_s = 0.75$ $K_s = 1.00$

(b)

$K_s = 0.00$ $K_s = 0.25$ $K_s = 0.50$ $K_s = 0.75$ $K_s = 1.00$

(c)

$K_s = 0.00$ $K_s = 0.25$ $K_s = 0.50$ $K_s = 0.75$ $K_s = 1.00$

(a)

(b)

(c)

Fig. 10 Comparisons of the AE count rate and deviatoric stress versus the elapsed time for the sandstone specimens with the confining pressure being 30 MPa and the water saturation coefficient being **a** 0.0, **b** 0.5, and **c** 1.0, respectively
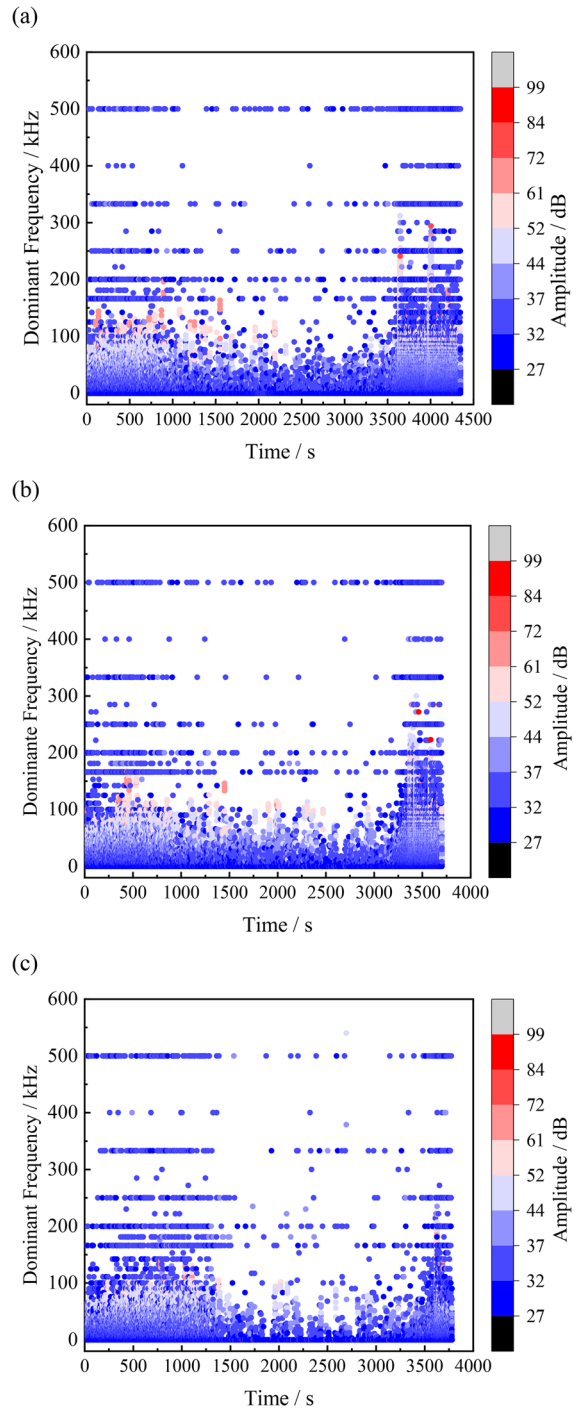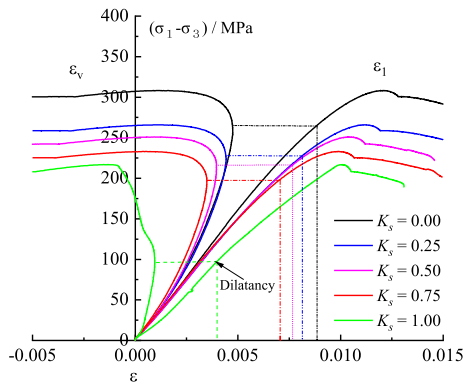
(a)

(b)

(c)

Fig. 11 Distributions of dominant frequency and amplitude of AE signals against the elapsed time for the sandstone specimens with the confining pressure being 30 MPa and the water saturation coefficient being **a** 0.0, **b** 0.5, and **c** 1.0, respectively

Fig. 12 Comparison of dilatancy behavior for the sandstone specimens with various water saturation coefficients from the triaxial unloading compression tests

an earlier onset of dilatancy for the $K_s = 1.0$ specimen. Given the fact that dissipation energy significantly increases during the period of dilatancy, the normalized dissipation energy for the $K_s = 1.0$ specimen tends to be larger, which is consistent with Fig. 8b. Therefore, the effect of moisture content on the onset of dilatancy of sandstones is insignificant for $K_s \leq 0.75$ specimens and significant for $K_s > 0.75$ specimens.

The extent of dilatancy during stage IV can be quantified by the crack volumetric strain (ε_v^{cr}) which is computed as follows (Nicksiar and Martin 2012):

$$\varepsilon_v^{cr} = \varepsilon_v^{tot} - \varepsilon_v^{el} \tag{7}$$

where ε_v^{tot} denotes the total volumetric strain; and ε_v^{el} represents the elastic volumetric strain which can be calculated by the following equation:

$$\varepsilon_v^{el} = \frac{2\mu - 1}{E}(\sigma_1 + 2\sigma_3) \tag{8}$$

Figure 13a, b, and c compares ε_v^{cr} curves for specimens with different K_s values. It shows that the increments of ε_v^{cr} during stage IV are 0.43%, 0.34%, and 0.17% for K_s values of 0.0, 0.5, and 1.0, respectively, indicating that increasing the water content significantly decreases the increment of ε_v^{cr}. This is, to some extent, consistent with Fig. 9. Specifically, increasing the water content suppresses the formation of tension fracture surfaces, thus decreasing the number and area of fracture surfaces (i.e., decrease of increment

of ε_v^{cr}). Therefore, increasing the water content would decrease the extent of dilatancy of sandstones.

3.5 Implications

The influences of moisture content on mechanical properties, failure characteristics, and dilatancy behavior of sandstone specimens have been studied in above subsections, which provides experimental bases for further understanding the role of moisture content in the rockburst intensity of sandstones. From a microscopic perspective, the initiation and propagation of micro-cracks are promoted by water due to the strain-softening behavior of clay minerals, the reduction of cohesion between grains, and the water wedge effect. Besides, the formation of tension micro-cracks is significantly suppressed when the water content is relatively high. Correspondingly, from a macro perspective, increasing the water content would significantly weaken the compressive strength of sandstones, which subsequently leads to a decrease of total strain energy. Moreover, as the water content increases, the number of tension fracture surfaces significantly decreases, indicating that a higher water content tends to yield a weaker brittleness of sandstones and thus a larger magnitude of normalized dissipation energy (Zhang et al. 2019b). According to Eq. (2), the elastic strain energy stored in sandstones would decrease with the increasing water content. In other words, the rockburst intensity of sandstones tends to decrease with the increase of moisture content.

4 Numerical investigation of a tunnel excavation case

To investigate the influence of moisture content on the rockburst intensity of tunnels during excavations, a numerical tunnel model is implemented in *RFPA*^{2D}. *RFPA*^{2D} is a numerical software for rock instability analysis, capable of reproducing the complex stress-deformation behavior of rocks before and after failure (Tian et al. 2021). Besides, the AE energy during the evolution of rock deformation and failure can also be simulated and displayed. The two-dimensional tunnel model with a length and width of 50 m is schematically shown in Fig. 14. The excavation chamber is a

Fig. 13 Comparison of crack volumetric strain as a function of axial strain for specimens with the water saturation coefficient being **a** 0.0, **b** 0.5, and **c** 1.0, respectively
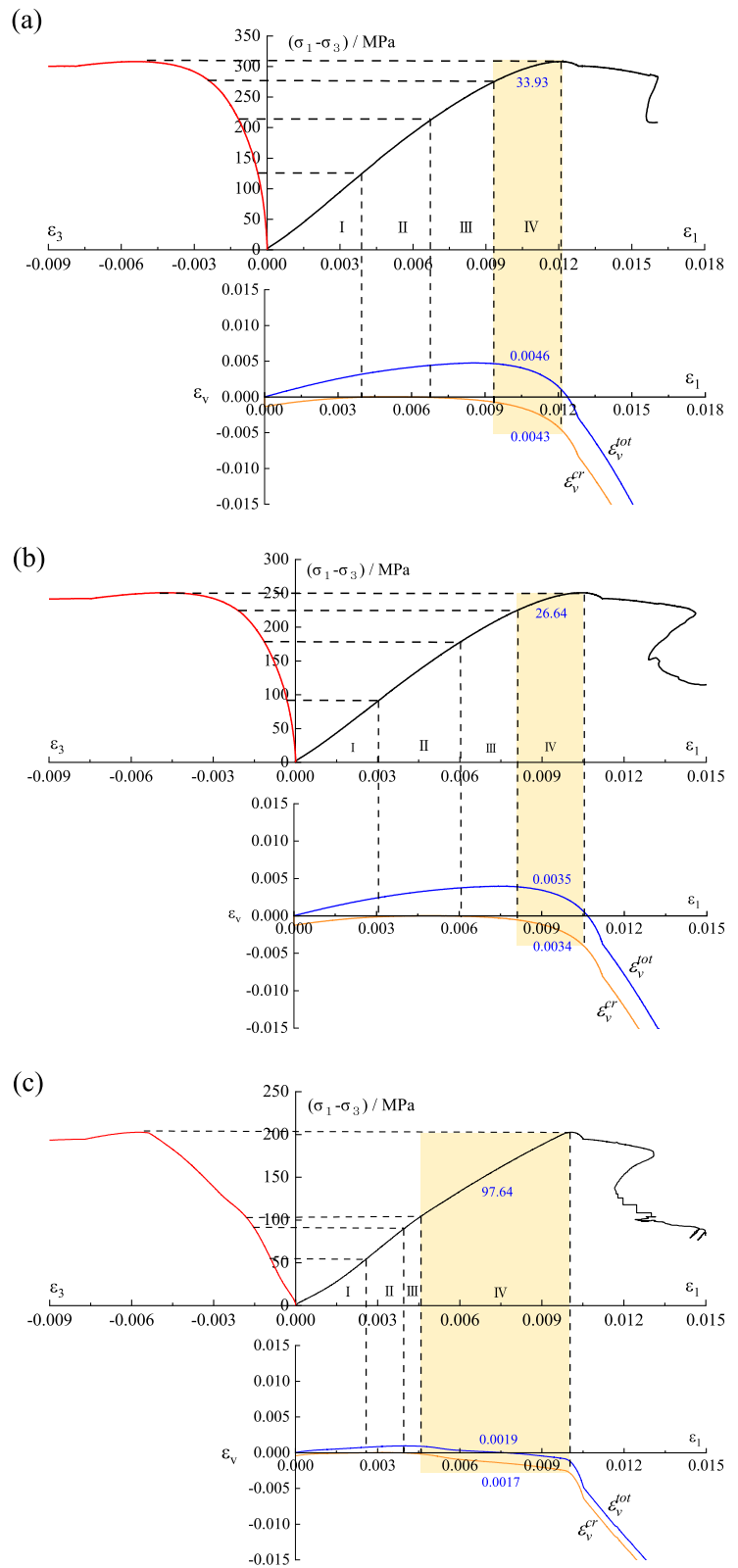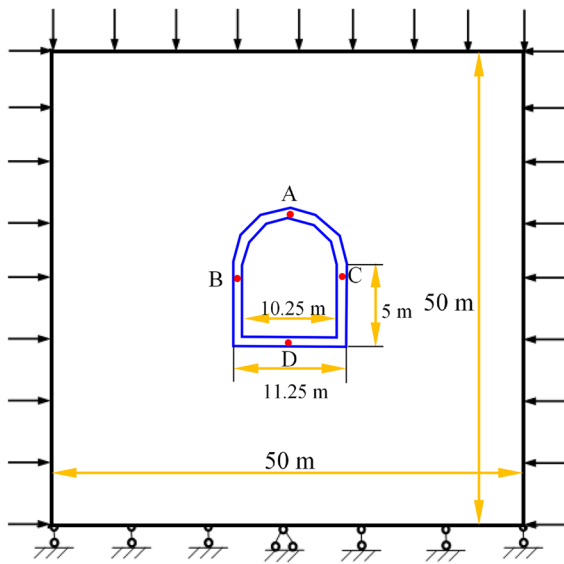
Fig. 14 Schematic representation of the tunnel model implemented

straight wall arch tunnel with a span of 10.25 m and a height of 5.0 m. It is assumed that only the 0.5 m thick surrounding rocks around the excavation chamber are affected by the water injection measure (see Fig. 1c) and the remaining surrounding rocks are dry materials. The sourrounding rocks consist of homogeneous sandstones, and the physical and mechanical parameters for the sandstones with different water content levels are tabulated in Table 2.

Totally five times of numerical simulations are performed, in order to consider five water-content levels of the 0.5 thick surrounding rocks, respectively. Each numerical simulation consists of two phases. In the first phase (i.e., generation of initial stress field), the bottom boundary surface is fixed; the gravitational acceleration is set as 9.81 m/s^2; a vertical stress with the magnitude of 45 MPa is applied on the top boundary surface, and a horizontal stress with the magnitude of 27 MPa is applied on both lateral boundary surfaces. Note that the magnitudes of

vertical and horizontal stresses consist of the gravity of overlying rock layers (Moomivand et al. 2022) as well as the tectonic stress. In the second phase (i.e., tunnel excavation), all elements in the excavation chamber are deleted, and the stress field of the tunnel model is redistributed accordingly. Trial calculations reveal that 9000 quadrilateral elements can guarantee sufficiently accurate simulations.

Figure 15 compares five excavation models in terms of contours of shear stress, maximum principal stress, and AE events. Note that these contours are automatically generated by *RFPA^{2D}*. In the subplots of AE events, the failure elements caused by tension and shear stresses are represented in red and white, respectively; and the AE events are represented by circles, and a larger circle denotes a higher magnitude of AE energy. Several observations can be made. First, the stresses within surrounding rocks are redistributed after excavations, and the stress concentration mainly occurs at both sides of the tunnel, thus resulting in the spalling of rock fragments (i.e., rockburst hazard). Second, the region of the rock fragments (i.e., intensity of rockburst hazard) is gradually reduced with increasing K_s values. This implies that the energy stored in sandstones decreases significantly with the increasing moisture content, which is consistent to the observations in Figs. 7 and 8. Third, the number of tension failure elements decreases with increasing K_s levels, indicating that the increasing water content suppresses the formation of tension fracture surfaces of sandstones. In other words, as observed in Fig. 9, the brittleness of surrounding rocks is weakened by the increase of water content. These observations confirm that the influence of water content on the rockburst intensity of sandstones is significant, and thus injecting water into the sandstone surrounding rocks is an effective way of reducing the intensity of rockburst hazards during tunnel excavations.

Table 2 Material parameters assigned to the sandstones with various water content levels	Water saturation coefficient	0.00	0.25	0.50	0.75	1.00
	Average compressive strength/MPa	172.31	132.24	126.35	122.07	103.59
	Elastic modulus/GPa	32.30	31.10	30.50	30.50	23.60
	Poisson's ratio	0.20	0.22	0.23	0.24	0.42
	Friction angle/°	44.70	44.80	43.20	41.50	40.50

Fig. 15 Contours of shear stress, maximum principal stress, and AE events for the tunnels with K_s of the 0.5 m thick surrounding rocks being **a** 0.0, **b** 0.25, **c** 0.50, **d** 0.75, and **e** 1.0, respectively. Note that the failure elements caused by tension and shear stresses are represented in red and white, respectively; and the AE events are represented by circles, and a larger circle denotes a higher magnitude of AE energy
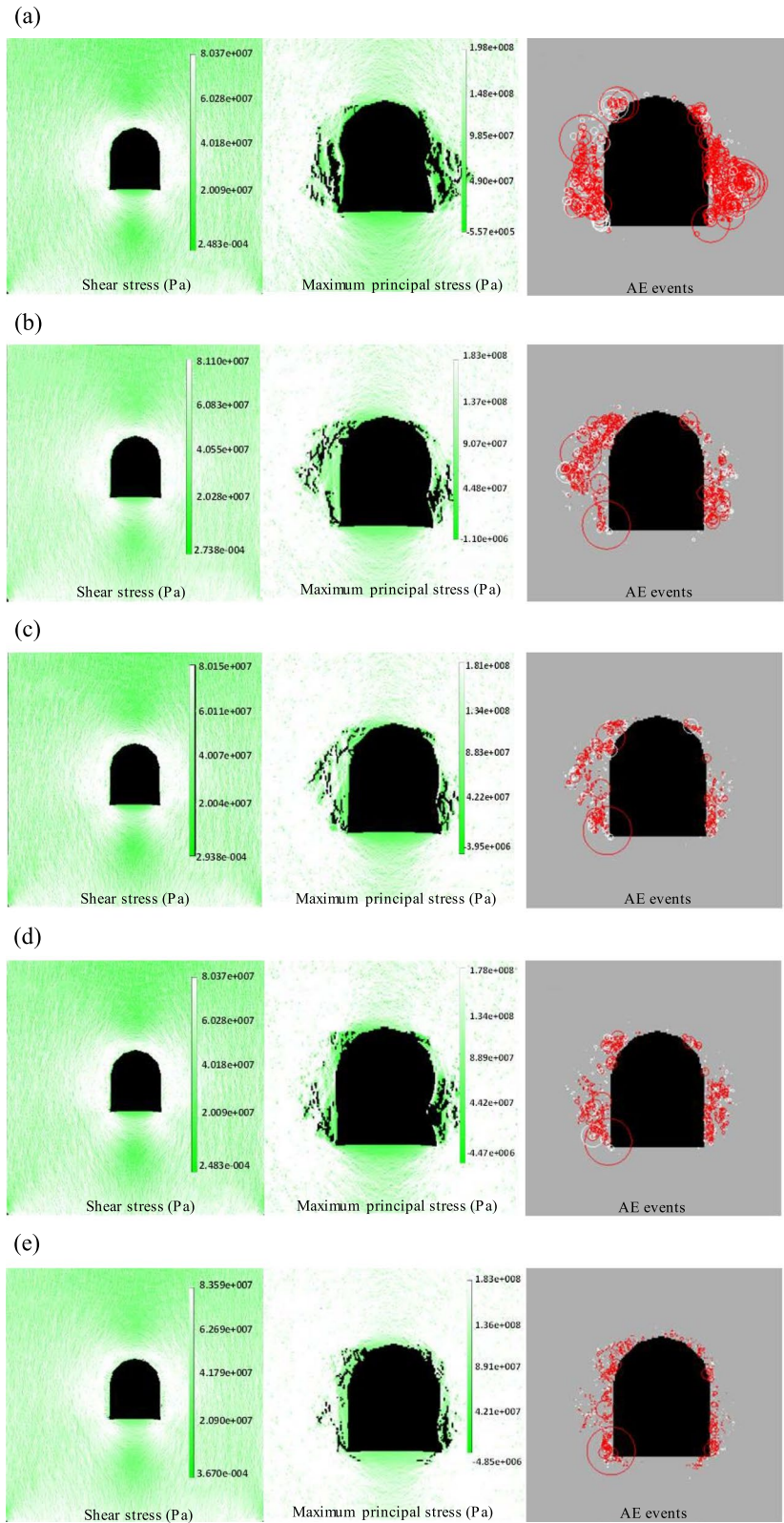
5 Conclusion

The influence of moisture content on the rockburst intensity of sandstones was systematically studied in this paper. All sandstone sepcimens were collected from Bamiao tunnel in Bazhong, Sichuan Province, China. After being processed into standard cylinders, these specimens were devided into 5 groups and the corresponding water saturation coefficient (K_s) levels were controlled to be 0.0, 0.25, 0.50, 0.75, and 1.0, respectively. For each group of specimens, three times of triaxial unloading compression tests were conducted under the confining stresses of 20 MPa, 30 MPa, and 40 MPa, respectively. In addition, numerical simulations of a tunnel excavation case given different moisture content levels were performed in $RFPA^{2D}$. Comparative results of laboratory experiments and numerical simulations lead to the following conclusions:

(1) Increasing the water content would decrease the compressive strength and increase Poisson's ratio of sandstones, which in turn yields a smaller magnitude of total strain energy. The compressive strength and total strain energy decrease by about 30% and 35%, respectively, when K_s changes from 0.0 to 1.0. Besides, a larger proportion of energy tends to be dissipated as the water content increases. Therefore, the magnitude of elastic strain energy, which is proportional to the rockburst intensity of sandstones, would decrease with the increasing water content.

(2) As the water content increases, the failure mode of sandstone specimens changes from a tension-shear composite failure to a shear failure, indicating that the brittleness of sandstones decreases with the increasing water content. In addition, the onset of dilatancy of sandstones is almost unaffected by the water content (except relatively high water content levels), whereas the extent of dilatancy of sandstones significantly decreases with the increasing water content.

(3) A higher water content level of the surrounding rocks around the excavation chamber tends to yield a smaller rockburst intensity of sandstones. It is thus evident that injecting water into the sandstone surrounding rocks is an effective way of reducing the intensity of rockburst hazards during tunnel excavations. The results provided can help engineers better understand the mechanism of moisture content effect on the rockburst intensity of sandstones.

Author contributions   Jiangchao Wang: Experiment, Methodology, Formal analysis, Writing-Original draft preparation. Wei Wang: Conceptualization, Validation, Supervision, Writing—Review and Editing. Guoqing Chen: Data curation, Supervision, Investigation. Yanke Wang: Experiment, Software, Suggestion.

Availability of data and materials   Data will be made available on request.

Declarations

Ethics approval and consent to participate
Not applicable.

References

Alkan H, Cinar Y, Pusch G (2007) Rock salt dilatancy boundary from combined acoustic emission and triaxial compression tests. Int J Rock Mech Min 44(1):108–119

Baud P, Zhu W, Wong TF (2000) Failure mode and weakening effect of water on sandstone. J Geophys Res-Solid Earth 105(B7):16371–16389. https://doi.org/10.1029/2000JB900087

Chen WZ, Lu SP, Guo XH, Qiao CJ (2009) Research on unloading confining pressure test and rockburst criterion based on energy theory. Chin J Rock Mech Eng 28(8):1530–1540 (**in Chinese**)

Chen GQ, Li TB, Wang W, Zhu ZF, Chen ZQ, Tang OL (2017a) Weakening effects of the presence of water on the brittleness of hard sandstone. Bull Eng Geol Environ 78(3):1471–1483. https://doi.org/10.1007/s10064-017-1184-3

Chen GQ, Li TB, Guo F, Wang YK (2017b) Brittle mechanical characteristics of hard rock exposed to moisture. Bull Eng Geol Environ 76(1):219–230. https://doi.org/10.1007/s10064-016-0857-7

Chen ZQ, He C, Ma GY, Xu GW, Ma CC (2019) Energy damage evolution mechanism of rock and its application to brittleness evaluation. Rock Mech Rock Eng 52(4):1265–1274. https://doi.org/10.1007/s00603-018-1681-0

Feng GL, Feng XT, Chen BR, Xiao YX, Yu Y (2015) A microseismic method for dynamic warning of rockburst development processes in tunnels. Rock Mech Rock Eng 48(5):2061–2076. https://doi.org/10.1007/s00603-014-0689-3

Feng XT, Hao XJ, Jiang Q, LiHudson SJJA (2016) Rock cracking indices for improved tunnel support design: a case study for columnar jointed rock masses. Rock Mech Rock Eng 49(6):2115–2130. https://doi.org/10.1007/s00603-015-0903-y

Feng XT, Gao YH, Zhang XW, Wang ZF, Zhang Y, Han Q (2020) Evolution of the mechanical and strength parameters of hard rocks in the true triaxial cyclic loading and unloading tests. Int J Rock Mech Min Sci. https://doi.org/10.1016/j.ijrmms.2020.104349

Gu L, Feng XT, Kong R, Yang C, Han Q, Xia Y (2023) Excavation stress path induced fracturing mechanism of hard rock in deep tunnel. Rock Mech Rock Eng 56:1779–1806. https://doi.org/10.1007/S00603-022-03151-9

Guo WY, Zhao TB, Tan YL, Yu FH, Hu SC (2017) Progressive mitigation method of rock bursts under complicated geological conditions. Int J Rock Mech Min 96:11–22. https://doi.org/10.1016/j.ijrmms.2017.04.011

Hawkins AB, McConnell BJ (1992) Sensitivity of sandstone strength and deformability to changes in moisture content. Q J Eng Geol Hydrogeol 25(2):115–130. https://doi.org/10.1144/GSL.QJEG.1992.025.02.05

Huang D, Li YR (2014) Conversion of strain energy in triaxial unloading tests on marble. Int J Rock Mech Min Sci 66:160–168. https://doi.org/10.1016/j.ijrmms.2013.12.001

Huang RQ, Wang XN, Chan LS (2001) Triaxial unloading test of rocks and its implication for rock burst. Bull Eng Geol Environ 60(1):37–41. https://doi.org/10.1007/s100640000082

Huang SB, He YB, Liu GF, Lu ZX, Xin ZK (2020) Effect of water content on the mechanical properties and deformation characteristics of the clay-bearing red sandstone. Bull Eng Geol Environ 80(2):1767–1790. https://doi.org/10.1007/s10064-020-01994-6

ISRM (2015) ISRM Suggested Methods For Rock Characterization, Testing and Monitoring: 2007–2014. Springer. https://doi.org/10.1007/s10064-015-0780-3

Kim E, Changani H (2016) Effect of water saturation and loading rate on the mechanical properties of red and buff sandstones. Int J Rock Mech Min 88:23–28. https://doi.org/10.1016/j.ijrmms.2016.07.005

Li D, Wong LNY, Liu G, Zhang X (2012a) Influence of water content and anisotropy on the strength and deformability of low porosity meta-sedimentary rocks under triaxial compression. Eng Geol 126:46–66. https://doi.org/10.1016/j.enggeo.2011.12.009

Li S, Feng XT, Li Z, Chen B, Zhang C, Hui Z (2012b) In situ monitoring of rockburst nucleation and evolution in the deeply buried tunnels of Jinping II hydropower station. Eng Geol 137–138:85–96. https://doi.org/10.1016/j.enggeo.2012.03.010

Li D, Sun Z, Xie T, Li X, Ranjith PG (2017) Energy evolution characteristics of hard rock during triaxial failure with different loading and unloading paths. Eng Geol 228:270–281. https://doi.org/10.1016/j.enggeo.2017.08.006

Liang WZ, Zhao GY, Wu H, Dai B (2019) Risk assessment of rockburst via an extended MABAC method under fuzzy environment. Tunn Undergr Space Technol 83:533–544. https://doi.org/10.1016/j.tust.2018.09.037

Liu X, Liang Z, Zhang Y, Liang P, Tian B (2018) Experimental study on the monitoring of rockburst in tunnels under dry and saturated conditions using ae and infrared monitoring. Tunn Undergr Sp Tech 82:517–528. https://doi.org/10.1016/j.tust.2018.08.011

Liu D, Sun J, Cao B, He M, Zhang Z, Peng D (2023) Experimental study on the effect and weakening mechanism of water on impact-induced rockburst. Chin J Rock Mech Eng 42(10):2441–2455 (**in Chinese**)

Lu AH, Hu SC, Li M, Duan TZ, Li B, Chang XY (2019) Impact of moisture content on the dynamic failure energy dissipation characteristics of sandstone. Shock Vib 6078342:1–10. https://doi.org/10.1155/2019/6078342

Luo Y (2020) Influence of water on mechanical behavior of surrounding rock in hard-rock tunnels: an experimental simulation. Eng Geol 277:105816. https://doi.org/10.1016/j.enggeo.2020.105816

Martin CD, Chandler NA (1994) The progressive fracture of Lac du Bonnet granite. Int J Rock Mech Min Sci Geomech Abstr 31(6):643–659. https://doi.org/10.1016/0148-9062(94)90005-1

Moomivand H, Moosazadeh S, Gilani SO (2022) A new empirical approach to estimate the ratio of horizontal to vertical in-situ stress and evaluation of its effect on the stability analysis of underground spaces. Rudarsko-Geološko-Naftni Zbornik 37(3):97–107

Nicksiar M, Martin CD (2012) Evaluation of methods for determining crack initiation in compression tests on

low-porosity rocks. Rock Mech Rock Eng 45(4):607–617. https://doi.org/10.1007/s00603-012-0221-6

Peng K, Zhou JQ, Zou QL, Zhang J, Wu F (2019) Effects of stress lower limit during cyclic loading and unloading on deformation characteristics of sandstones. Constr Build Mater 217:202–215. https://doi.org/10.1016/j.conbuildmat.2019.04.183

Shen RX, Li HR, Wang EY, Chen TQ, Li TX, Tian H, Hou ZH (2020) Infrared radiation characteristics and fracture precursor information extraction of loaded sandstone samples with varying moisture contents. Int J Rock Mech Min Sci. https://doi.org/10.1016/j.ijrmms.2020.104344

Song DZ, Wang EY, Liu ZT, Liu XF, Shen RX (2014) Numerical simulation of rock-burst relief and prevention by water-jet cutting. Int J Rock Mech Min Sci 70:318–331. https://doi.org/10.1016/j.ijrmms.2014.05.015

Tang SB (2018) The effects of water on the strength of black sandstone in a brittle regime. Eng Geol 239:167–178. https://doi.org/10.1016/j.enggeo.2018.03.025

Tang SB, Yu CY, Tang CA (2018) Numerical modeling of the time-dependent development of the damage zone around a tunnel under high humidity conditions. Tunn Undergr Space Technol 76:48–63. https://doi.org/10.1016/j.tust.2018.03.012

Tian ZC, Tang CN, Li H, Xing H, Ning XD (2021) Numerical simulation of rock uniaxial compressive strength and deformation failure law under different size conditions. Adv Civ Eng 2:1–11. https://doi.org/10.1155/2021/6643884

Vásárhelyi B, Ván P (2006) Influence of water content on the strength of rock. Eng Geol 84(1):70–74. https://doi.org/10.1016/j.enggeo.2005.11.011

Wang G, Gong S, Dou L, Cai W, Yuan X, Fan C (2019) Rock-burst mechanism and control in coal seam with both syncline and hard strata. Saf Sci 115:320–328. https://doi.org/10.1016/j.ssci.2019.02.020

Wong LNY, Maruvanchery V, Liu G (2016) Water effects on rock strength and stiffness degradation. Acta Geotech 11(4):713–737. https://doi.org/10.1007/s11440-015-0407-7

Xiao YX, Feng XT, Li SJ, Feng GL, Yu Y (2016) Rock mass failure mechanisms during the evolution process of rock-bursts in tunnels. Int J Rock Mech Min Sci 83:174–181. https://doi.org/10.1016/j.ijrmms.2016.01.008

Xue JH, Du XH, Ma Q, Zhan KL (2021) Experimental study on law of limit storage energy of rock under different confining pressures. Arab J Geosci 14(1):62. https://doi.org/10.1007/s12517-020-06398-0

Yang Y, Xie H, Xiao M, He J (2017) Dilatancy and energy characteristics analysis of transverse-isotropic rock mass under triaxial unloading condition. Rock Soil Mech 38(6):1589–1599 (**in Chinese**)

Yuan SC, Harrison JP (2004) An empirical dilatancy index for the dilatant deformation of rock. Int J Rock Mech Min 41(4):679–686. https://doi.org/10.1016/j.ijrmms.2003.11.001

Zhang CQ, Feng XT, Zhou H, Qiu SL, Wu WP (2012) Case histories of four extremely intense rockbursts in deep tunnels. Rock Mech Rock Eng 45(3):275–288. https://doi.org/10.1007/s00603-011-0218-6

Zhang Y, Feng X, Yang C, Zhang X, Sharifzadeh M, Wang Z (2019a) Fracturing evolution analysis of beishan granite under true triaxial compression based on acoustic emission and strain energy. Int J Rock Mech Min 117:150–161. https://doi.org/10.1016/j.ijrmms.2019.03.029

Zhang Y, Feng XT, Zhang XW, Wang ZF, Sharifzadeh M, Yang CX (2019b) A novel application of strain energy for fracturing process analysis of hard rock under true triaxial compression. Rock Mech Rock Eng 52(11):4257–4272. https://doi.org/10.1007/s00603-019-01868-8

Zhou H, Meng FZ, Zhang CQ, Hu DW, Yang FJ, Lu JJ (2015) Analysis of rockburst mechanisms induced by structural planes in deep tunnels. Bull Eng Geol Environ 74(4):1435–1451. https://doi.org/10.1007/s10064-014-0696-3

Zhou ZL, Cai X, Ma D, Cao WZ, Chen L, Zhou J (2018) Effects of water content on fracture and mechanical behavior of sandstone with a low clay mineral content. Eng Fract Mech 193:47–65. https://doi.org/10.1016/j.engfracmech.2018.02.028

Zhu QH, Lu WB, Sun JS (2007) Discussion on mechanism of rockburst and stress state based on energy principles. Jwuhan Univ 40(2):84–87 (**in Chinese**)